GLOBAL BIFURCATIONS CLOSE TO SYMMETRY

ISABEL S. LABOURIAU ALEXANDRE A. P. RODRIGUES

Abstract. This article treats the dynamics around a heteroclinic cycle involving two saddle-foci, where the saddle-foci share both invariant manifolds. This type of cycle occurs generically in symmetric differential equations on the 3-dimensional sphere. We study the case when trajectories near the two equilibria turn in the same direction around the 1-dimensional connection — the saddle-foci have the same chirality.

When part of the symmetry is broken, the 2-dimensional invariant manifolds intersect transversely creating a heteroclinic network of Bykov cycles. We show that this creates heteroclinic tangencies that coexist with hyperbolic dynamics. There are n-pulse heteroclinic tangencies — trajectories that follow the original cycle n times around before they arrive at the other node. Each n-pulse heteroclinic tangency is accumulated by a sequence of $n+1$-pulse ones. This coexists with the suspension of horseshoes defined on an infinite set of disjoint strips, where the dynamics is hyperbolic. We also show how, as the system approaches full symmetry, the suspended horseshoes are destroyed, creating regions with infinitely many attracting periodic orbits.

1. Introduction

A Bykov cycle is a heteroclinic cycle between two hyperbolic saddle-foci of different Morse index, where one of the connections is transverse and the other is structurally unstable — see Figure 1. There are two types of Bykov cycle, depending on the way the flow turns around the two saddle-foci, that determine the *chirality* of the cycle. Here we study the non-wandering dynamics in the neighbourhood of a Bykov cycle where the two nodes have the same chirality. This is also studied in [21], and the case of different chirality is discussed in [23].

Our starting point is a fully symmetric system $\dot{x} = f_0(x)$ with two saddle-foci that share all the invariant manifolds, of dimensions one and two, both contained in flow-invariant subspaces that come from the symmetry. This forms an attracting heteroclinic network Σ^0 with a non-empty basin of attraction V^0. We study the global transition of the dynamics from this fully symmetric system $\dot{x} = f_0(x)$ to a perturbed system $\dot{x} = f_\lambda(x)$, for a smooth one-parameter family that breaks some of the symmetry of the system. For small perturbations the set V^0 is still positively invariant.

When $\lambda \neq 0$, the one-dimensional connection persists, due to the remaining symmetry, and the two dimensional invariant manifolds intersect transversely, because of the symmetry breaking. This gives rise to a network Σ^λ, that consists of a union of Bykov cycles, contained in V^0. For partial symmetry-breaking perturbations of f_0, we are interested in the dynamics in $\Omega(V_0)$, the maximal invariant set contained in V^0. It contains, but does not coincide with, the suspension of horseshoes accumulating on Σ^λ, as shown in [2, 21, 19]. Here, we show that close to the fully

Date: April 8, 2015.

2010 *Mathematics Subject Classification.* Primary: 34C28 Secondary: 34C37, 37C29, 37D05, 37G35.

Key words and phrases. Heteroclinic tangencies, Non-hyperbolicity, Symmetry breaking, Global bifurcations, Routes to chaos.

CMUP is supported by the European Regional Development Fund through the programme COMPETE and by the Portuguese Government through the Fundação para a Ciência e a Tecnologia (FCT) under the project PEst-C/MAT/UI0144/2011. A.A.P. Rodrigues was supported by the grant SFRH/BPD/84709/2012 of FCT.

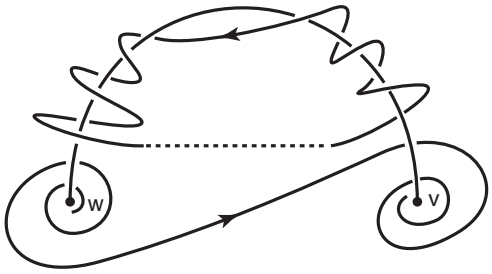

FIGURE 1. A Bykov cycle with nodes of the same chirality. There are two possibilities for the geometry of the flow around a Bykov cycle depending on the direction trajectories turn around the connection $[\mathbf{v} \to \mathbf{w}]$. We assume here that the nodes have the same chirality: trajectories turn in the same direction around the connection. When the endpoints of a nearby trajectory are joined, the closed curve is always linked to the cycle.

symmetric case it also contains infinitely many heteroclinic tangencies. Under an additional assumption we show that $\Omega(V_0)$ also contains attracting limit cycles with long periods.

Symmetry plays two roles here. First, it creates flow-invariant subspaces where non-transverse heteroclinic connections are persistent, and hence Bykov cycles are robust in this context. Second, being close to a more symmetric problem organises the information and imposes some restrictions on the invariant manifolds of the saddle-foci, and this is the origin of the heteroclinic tangencies and related bifurcations.

Cycles where the two nodes have the same chirality are addressed by Knobloch *et al* [19]. They restrict the analysis to trajectories that remain for all time inside a small tubular neighbourhood of the cycle. With this constraint they find that there are at most two heteroclinic tangencies, and that they only occur if the ratio of the real parts of the complex eigenvalues is irrational. We use the proximity of the fully symmetric case to capture more global dynamics, and we find infinitely many heteroclinic tangencies corresponding to trajectories that make an excursion away from the original cycle. In contrast, around Bykov cycles where the nodes have different chirality, heteroclinic tangencies occur generically in trajectories that remain close to the cycle for all time, as shown in [23]. Chirality is an essential information in this problem.

Homoclinic and heteroclinic bifurcations constitute the core of our understanding of complicated recurrent behaviour in dynamical systems. The history goes back to Poincaré on the late 19^{th} century, with major subsequent contributions by the schools of Andronov, Shilnikov, Smale and Palis. These results rely on a combination of analytical and geometrical tools used to understand the qualitative behaviour of the dynamics.

Heteroclinic cycles and networks are flow-invariant sets that can occur robustly in dynamical systems with symmetry, and are frequently associated with intermittent behaviour. The rigorous analysis of the dynamics associated to the structure of the nonwandering sets close to heteroclinic networks is still a challenge. We refer to [16] for an overview of heteroclinic bifurcations and for details on the dynamics near different kinds of heteroclinic cycles and networks. In the present article, we study the non-wandering dynamics in the neighbourhood of a Bykov cycle.

Bykov cycles appear in many applications like the Kuramoto-Sivashinsky systems [9, 24], magnetoconvection [34] and travelling waves in reaction-diffusion dynamics [5]. In generic dynamical systems heteroclinic cycles are invariant sets of codimension one, but they can be structurally stable in systems which are equivariant under the action of a symmetry group, due to the existence of flow-invariant subspaces. Explicit examples of equivariant vector fields for which such cycles may be found are reported in [3, 4, 18, 23, 25, 30, 33].

The transverse intersection of the two-dimensional invariant manifolds of the two nodes implies that the set of trajectories that remain for all time in a small neighbourhood of the Bykov cycle contains a locally-maximal hyperbolic set admitting a complete description in terms of symbolic dynamics, reminiscent of the results of L.P. Shilnikov [37]. An obstacle to the global symbolic description of these trajectories is the existence of tangencies that lead to the birth of stable periodic sinks, as described for the homoclinic case in [1, 27, 28, 39]. In the present article, we prove that when $\lambda \to 0$, the horseshoes in $\Omega(V^0)$ lose hyperbolicity at heteroclinic tangencies with Newhouse phenomena. The complete description is an unsolvable problem: arbitrarily small perturbations of any differential equation with a quadratic heteroclinic tangency may lead to the creation of new tangencies of higher order, and to the birth of degenerate periodic solutions [14, §4]. See also the article [17], about the existence of generic cubic homoclinic tangencies in the context of Hénon maps.

All dynamical models with quasi-stochastic attractors were found, either analytically or by computer simulations, to have tangencies of invariant manifolds [1, 12, 13]. As a rule, the sinks in a quasi-stochastic attractor have very long periods and narrow basins of attraction, and they are hard to observe in applied problems because of the presence of noise, see [14].

The present article contributes to a better understanding of the global transition between uniform hyperbolicity (Smale horseshoes with infinitely many strips) coexisting with infinitely many sinks, and the emergence of regular dynamics. We discuss the global bifurcations that occur as a parameter λ is used to break part of the symmetry. We complete our results by reducing our problem to a symmetric version of the structure of Palis and Takens' result [29, §3] on homoclinic bifurcations. Being close to symmetry adds complexity to the dynamics.

Framework of the article. This article is organised as follows. In Section 2, after some basic definitions, we describe precisely the object of study and we review some of our recent results related to it. In Section 3 we state the main results of the present article. The coordinates and other notation used in the rest of the article are presented in Section 4, where we also obtain a geometrical description of the way the flow transforms a curve of initial conditions lying across the stable manifold of an equilibrium. In Section 5, we prove that there is a sequence of parameter values λ_i accumulating on 0 such that the associated flow has heteroclinic tangencies. In Section 6, we discuss the geometric constructions that describe the global dynamics near a Bykov cycle as the parameter varies. We also describe the limit set that contains nontrivial hyperbolic subsets and we explain how the horseshoes disappear as the system regains full symmetry. We show that under an additional condition this creates infinitely many attracting periodic solutions.

2. The object of study and preliminary results

In the present section, after some preliminary definitions, we state the hypotheses for the system under study together with an overview of results obtained in [21], emphasizing those that will be used to explain the loss of hyperbolicity of the suspended horseshoes and the emergence of heteroclinic tangencies near the cycle.

2.1. **Definitions.** Let f be a C^2 vector field on $\mathbf{R}^n$ with flow given by the unique solution $x(t) = \varphi(t, x_0) \in \mathbf{R}^n$ of

$$\dot{x} = f(x) \qquad \text{and} \qquad x(0) = x_0.$$

Given two equilibria p_1 and p_2, an m-dimensional *heteroclinic connection* from p_1 to p_2, denoted $[p_1 \to p_2]$, is an m-dimensional connected flow-invariant manifold contained in $W^u(p_1) \cap W^s(p_2)$. There may be more than one trajectory connecting p_1 and p_2.

Let $S = \{p_j : j \in \{1, \dots, k\}\}$ be a finite ordered set of equilibria. There is a *heteroclinic cycle* associated to S if

$$\forall j \in \{1, \dots, k\}, W^u(p_j) \cap W^s(p_{j+1}) \neq \emptyset \pmod k,$$

where $W^s(p)$ and $W^u(p)$ refer to the stable and unstable manifolds of the hyperbolic saddle p, respectively. A *heteroclinic network* is a finite connected union of heteroclinic cycles. The dimension of the unstable manifold of an equilibrium p will be called the *Morse index* of p.

These objects are known to exist in several settings and are structurally stable within certain classes of Γ-equivariant systems, where $\Gamma \subset \mathbf{O}(n)$ is a compact Lie group. Here we consider differential equations $\dot{x} = f(x)$ with the equivariance condition:

$$f(\gamma x) = \gamma f(x), \qquad \text{for all } \gamma \in \Gamma.$$

Given an isotropy subgroup $\widetilde{\Gamma} < \Gamma$, we write $Fix(\widetilde{\Gamma})$ for the vector subspace of points that are fixed by the elements of $\widetilde{\Gamma}$. For Γ-equivariant differential equations each subspace $Fix(\widetilde{\Gamma})$ is flow-invariant.

In a three-dimensional manifold, a *Bykov cycle* is a heteroclinic cycle associated to two hyperbolic saddle-foci with different Morse indices, in which the one-dimensional manifolds coincide and the two-dimensional invariant manifolds have a transverse intersection. The dynamics near this kind of cycles has recently been studied in the reversible context by [9, 10, 19, 24] and in the equivariant setting by [21]. See also [11, 32].

Suppose there is a cross-section S to the flow of $\dot{x} = f(x)$, such that S contains a compact invariant set Λ where the first return map is well defined and conjugate to a full shift on a countable alphabet. A *suspended horseshoe* is a flow-invariant set $\widetilde{\Lambda} = \{\varphi(t, q) : t \in \mathbf{R}, q \in \Lambda\}$.

2.2. **The organising centre.** The starting point of the analysis is a differential equation $\dot{x} = f_0(x)$ on the unit sphere $\mathbf{S}^3 = \{X = (x_1, x_2, x_3, x_4) \in \mathbf{R}^4 : ||X|| = 1\}$ where $f_0 : \mathbf{S}^3 \to \mathbf{TS}^3$ is a C^2 vector field with the following properties:

(P1) The vector field f_0 is equivariant under the action of $\mathbf{Z}_2 \oplus \mathbf{Z}_2$ on $\mathbf{S}^3$ induced by the linear maps on $\mathbf{R}^4$:

$$\gamma_1(x_1, x_2, x_3, x_4) = (-x_1, -x_2, x_3, x_4) \qquad \text{and} \qquad \gamma_2(x_1, x_2, x_3, x_4) = (x_1, x_2, -x_3, x_4).$$

(P2) The set $Fix(\mathbf{Z}_2 \oplus \mathbf{Z}_2) = \{x \in \mathbf{S}^3 : \gamma_1 x = \gamma_2 x = x\}$ consists of two equilibria $\mathbf{v} = (0, 0, 0, 1)$ and $\mathbf{w} = (0, 0, 0, -1)$ that are hyperbolic saddle-foci, where:
- the eigenvalues of $df_0(\mathbf{v})$ are $-C_\mathbf{v} \pm \alpha_\mathbf{v} i$ and $E_\mathbf{v}$ with $\alpha_\mathbf{v} \neq 0$, $C_\mathbf{v} > E_\mathbf{v} > 0$;
- the eigenvalues of $df_0(\mathbf{w})$ are $E_\mathbf{w} \pm \alpha_\mathbf{w} i$ and $-C_\mathbf{w}$ with $\alpha_\mathbf{w} \neq 0$, $C_\mathbf{w} > E_\mathbf{w} > 0$.

(P3) The flow-invariant circle $Fix(\langle\gamma_1\rangle) = \{x \in \mathbf{S}^3 : \gamma_1 x = x\}$ consists of the two equilibria $\mathbf{v}$ and $\mathbf{w}$, a source and a sink, respectively, and two heteroclinic trajectories from $\mathbf{v}$ to $\mathbf{w}$ that we denote by $[\mathbf{v} \to \mathbf{w}]$.

(P4) The f_0-invariant sphere $Fix(\langle\gamma_2\rangle) = \{x \in \mathbf{S}^3 : \gamma_2 x = x\}$ consists of the two equilibria $\mathbf{v}$ and $\mathbf{w}$, and a two-dimensional heteroclinic connection from $\mathbf{w}$ to $\mathbf{v}$. Together with the connections in (P3) this forms a heteroclinic network that we denote by Σ^0.

Given two small open neighbourhoods V and W of $\mathbf{v}$ and $\mathbf{w}$ respectively, consider a piece of trajectory φ that starts at ∂V, goes into V and then goes once from V to W, ending at ∂W. Joining the starting point of φ to its end point by a line segment, one obtains a closed curve, the *loop* of φ. For almost all starting positions in ∂V, the loop of φ does not meet the network Σ^0. If there are arbitrarily small neighbourhoods V and W for which the loop of every trajectory is linked to Σ_0, we say that *the nodes have the same chirality* as ilustrated in Figure 1. This means that near $\mathbf{v}$ and $\mathbf{w}$, all trajectories turn in the same direction around the one-dimensional connections $[\mathbf{v} \to \mathbf{w}]$. This is our last hypothesis on f_0:

(P5) The saddle-foci $\mathbf{v}$ and $\mathbf{w}$ have the same chirality.

Condition (P5) means that the curve φ and the cycle Σ^0 cannot be separated by an isotopy. This property is persistent under small smooth perturbations of the vector field that preserve the one-dimensional connection. An explicit example of a family of differential equations where this assumption is valid has been constructed in [33]. The rigorous analysis of a case where property (P5) does not hold has been done in [23].

2.3. **The heteroclinic network of the organising centre.** The heteroclinic connections in the network Σ^0 are contained in fixed point subspaces satisfying the hypothesis (H1) of Krupa and Melbourne [20]. Since the inequality $C_{\mathbf{v}}C_{\mathbf{w}} > E_{\mathbf{v}}E_{\mathbf{w}}$ holds, the stability criterion [20] may be applied to Σ^0 and we have:

Lemma 1. *Under conditions (P1)–(P4) the heteroclinic network Σ^0 is asymptotically stable.*

As a consequence of Lemma 1 there exists an open neighbourhood V^0 of the network Σ^0 such that every trajectory starting in V^0 remains in it for all positive time and is forward asymptotic to the network. The neighbourhood may be taken to have its boundary transverse to the vector field f_0. The flow associated to any C^1-perturbation of f_0 that breaks the one-dimensional connection should have some attracting feature. When the symmetry $\mathbf{Z}_2(\langle\gamma_1\rangle)$ is broken, the two one-dimensional heteroclinic connections are destroyed and the cycle Σ^0 disappears. Each cycle is replaced by a hyperbolic sink that lies close to the original cycle [21]. For sufficiently small C^1-perturbations, the existence of solutions that go several times around the cycles is ruled out.

The fixed point hyperplane defined by $Fix(\langle\gamma_2\rangle) = \{(x_1, x_2, x_3, x_4) \in \mathbf{S}^3 : x_3 = 0\}$ divides $\mathbf{S}^3$ in two flow-invariant connected components, preventing arbitrarily visits to both cycles in Σ^0. Trajectories whose initial condition lies outside the invariant subspaces will approach one of the cycles in positive time. Successive visits to both cycles require breaking this symmetry [21].

2.4. **Breaking the $\mathbf{Z}_2(\langle\gamma_2\rangle)$-symmetry.** From now on, we consider f_0 embedded in a generic one-parameter family of vector fields, breaking the $\langle\gamma_2\rangle$-equivariance as follows:

(P6) The vector fields $f_\lambda : \mathbf{S}^3 \to \mathbf{TS}^3$ are a C^1-family of $\langle\gamma_1\rangle$-equivariant vector fields.

Since the equilibria $\mathbf{v}$ and $\mathbf{w}$ lie on $Fix(\langle\gamma_1\rangle)$ and are hyperbolic, they persist for small $\lambda > 0$ and still satisfy Properties (P2) and (P3). Their invariant two-dimensional manifolds generically meet transversely. The generic bifurcations from a manifold are discussed in [7], under these conditions we assume:

(P7) For $\lambda \neq 0$, the local two-dimensional manifolds $W^u(\mathbf{w})$ and $W^s(\mathbf{v})$ intersect transversely at two trajectories that will be denoted $[\mathbf{v} \to \mathbf{w}]$. Together with the connections in (P3) this forms a Bykov heteroclinic network that we denote by Σ^λ.

The network Σ^λ consists of four copies of the simplest heteroclinic cycle between two saddle-foci of different Morse indices, where one heteroclinic connection is structurally stable and the other is not, a *Bykov cycle*.

The next result shows that Property (P7) is natural, since the heteroclinic connections of (P7), as well as those of assertion (4) of Theorem 3 below, occur at least in symmetric pairs.

Lemma 2. *Let f_λ be a C^1-family of vector fields satisfying (P1)–(P3) and (P6). If the local two-dimensional manifolds $W^u(\mathbf{w})$ and $W^s(\mathbf{v})$ intersect at a point then their intersection contains at least two trajectories.*

Proof. Let $x(t)$ be a solution of $\dot{x} = f_\lambda(x)$ with $x(0)$ contained in $W^u_{loc}(\mathbf{w}) \cap W^s_{loc}(\mathbf{v})$, hence $x(t) \in W^u_{loc}(\mathbf{w}) \cap W^s_{loc}(\mathbf{v})$ for all t. Then $\gamma_1 x(t)$ is also a solution with the same property. If $\gamma_1 x(t) = x(t)$, then $x(t) \in Fix(\langle\gamma_1\rangle)$ contradicting $(P3)$. □

For small $\lambda \neq 0$, the neighbourhood V^0 is still positively invariant and contains the network Σ^λ. Since the closure of V^0 is compact and positively invariant it contains the ω-limit sets of all its trajectories. The union of these limit sets is a maximal invariant set in V^0. For f_0 this is the cycle Σ^0, by Lemma 1, whereas for symmetry-breaking perturbations of f_0 it contains Σ^λ but does not coincide with it. Our aim is to describe this set.

When λ moves away from 0, the simple dynamics jumps to chaotic behaviour. A systematic study of the dynamics in a neighbourhood of the Bykov cycles in Σ^λ, under the condition (P5), was carried out in [2, 21, 22]; we proceed to review these local results and then we discuss global aspects of the dynamics. In order to do this we introduce some concepts.

Given a Bykov cycle Γ involving $\mathbf{v}$ and $\mathbf{w}$, let $V, W \subset V^0$ be disjoint neighbourhoods of these points as above. Consider two local cross-sections of Σ^λ at two points p and q in the connections $[\mathbf{v} \to \mathbf{w}]$ and $[\mathbf{w} \to \mathbf{v}]$, respectively, with $p, q \notin V \cup W$. Saturating the cross-sections by the flow, one obtains two flow-invariant tubes joining V and W that contain the connections in their interior. We call the union of these tubes with V and W a *tubular neighbourhood* $\mathcal{T}$ of the Bykov cycle. More details will be provided in Section 4.

Given two disjoint neighbourhoods V and $W \subset V^0$ of $\mathbf{v}$ and $\mathbf{w}$, respectively, a one-dimensional connection $[\mathbf{w} \to \mathbf{v}]$ that, after leaving W, enters and leaves both V and W precisely $n \in \mathbf{N}$ times is called an *n-pulse heteroclinic connection* with respect to V and W. When there is no ambiguity, we omit the expression "with respect to V and W". If $n \geq 1$ we call it a *multi-pulse heteroclinic connection*. If $W^u(\mathbf{w})$ and $W^s(\mathbf{v})$ meet tangentially, we say that the connection $[\mathbf{w} \to \mathbf{v}]$ is an *n-pulse heteroclinic tangency*, otherwise we call it a *transverse n-pulse heteroclinic connection*. The original heteroclinic connections $[\mathbf{w} \to \mathbf{v}]$ in Σ^λ are 0-pulse heteroclinic connections.

With these conventions we have:

Theorem 3 ([21])**.** *If a vector field f_0 satisfies (P1)–(P5), then the following properties are satisfied generically by vector fields in an open neighbourhood of f_0 in the space of $\langle\gamma_1\rangle$-equivariant vector fields of class C^1 on $\mathbf{S}^3$:*

1. *there is a heteroclinic network Σ^* consisting of four Bykov cycles involving two equilibria $\mathbf{v}$ and $\mathbf{w}$, two 0-pulse heteroclinic connections $[\mathbf{v} \to \mathbf{w}]$ and two 0-pulse heteroclinic connections $[\mathbf{w} \to \mathbf{v}]$;*
2. *the only heteroclinic connections from $\mathbf{v}$ to $\mathbf{w}$ are those in the Bykov cycles and there are no homoclinic connections;*
3. *any tubular neighbourhood $\mathcal{T}$ of a Bykov cycle Γ in Σ^* contains points not lying on Γ whose trajectories remain in $\mathcal{T}$ for all time;*
4. *any tubular neighbourhood of a Bykov cycle Γ in Σ^* contains infinitely many n-pulse heteroclinic connections $[\mathbf{w} \to \mathbf{v}]$ for each $n \in \mathbf{N}$, that accumulate on the cycle;*
5. *for any tubular neighbourhood $\mathcal{T}$, given a cross-section $S_q \subset \mathcal{T}$ at a point q in $[\mathbf{w} \to \mathbf{v}]$, there exist sets of points such that the dynamics of the first return to S_q is uniformly hyperbolic and conjugate to a full shift over a finite number of symbols. These sets accumulate on Σ^* and the number of symbols coding the return map tends to infinity as we approach the network.*

Notice that assertion (4) of Theorem 3 implies the existence of a bigger network: beyond the original transverse connections $[\mathbf{w} \to \mathbf{v}]$, there exist infinitely many subsidiary heteroclinic connections turning around the original Bykov cycle. Hereafter, we will restrict our study to one heteroclinic cycle.

The results of L.P. Shilnikov on a homoclinic cycle to a saddle-focus [36, 37, 38] are well known. Under a specific eigenvalue condition the cycle gives rise to an invariant set where the first return map is conjugate to a full shift over a finite alphabet. In contrast to these findings,

in Theorem 3, the suspended horseshoes arise due to the presence of two saddle-foci together with transversality of invariant manifolds, and does not depend on any additional condition on the eigenvalues at the nodes.

A hyperbolic invariant set of a C^2-diffeomorphism has zero Lebesgue measure [6]. Nevertheless, since the authors of [21] worked in the C^1 category, this set of horseshoes might have positive Lebesgue measure. Rodrigues [31] proved that this is not the case:

Theorem 4 ([31])**.** *Let $\mathcal{T}$ be a tubular neighbourhood of one of the Bykov cycles Γ of Theorem 3. Then in any cross-section $S_q \subset \mathcal{T}$ the set of initial conditions in S_q that do not leave $\mathcal{T}$ for all time, has zero Lebesgue measure.*

The shift dynamics does not trap most solutions in the neighbourhood of the cycle. In particular, none of the cycles is Lyapunov stable.

3. Statement of results

Heteroclinic cycles connecting saddle-foci with a transverse intersection of two-dimensional invariant manifolds imply the existence of hyperbolic suspended horseshoes. In our setting, when λ varies close to zero, we expect the creation and the annihilation of these horseshoes. When the symmetry $\mathbf{Z}_2(\langle\gamma_2\rangle)$ is broken, heteroclinic tangencies are reported in the next result. Although a tangency may be removed by a small smooth perturbation, the presence of tangencies is persistent.

Theorem 5. *In the set of families f_λ of vector fields satisfying (P1)–(P6) there is a subset $\mathcal{C}$, open in the C^2 topology, for which there is a sequence $\lambda_i > 0$ of real numbers, with $\lim_{i\to\infty} \lambda_i = 0$ such that for $\lambda > \lambda_i$, there are two 1-pulse heteroclinic connections for the flow of $\dot{x} = f_\lambda(x)$, that collapse into a 1-pulse heteroclinic tangency at $\lambda = \lambda_i$ and then disappear for $\lambda < \lambda_i$. Moreover, the 1-pulse heteroclinic tangency approaches the original $[\mathbf{w} \to \mathbf{v}]$ connection when λ_i tends to zero.*

The explicit description of the open set $\mathcal{C}$ is given in Section 5, after establishing some notation for the proof.

Theorem 6. *For a family f_λ in the open set $\mathcal{C}$ of Theorem 5, and for each parameter value λ_i corresponding to a 1-pulse heteroclinic tangency, there is a sequence of parameter values λ_{ij} accumulating at λ_i for which there is a 2-pulse heteroclinic tangency. This property is recursive in the sense that each n-pulse heteroclinic tangency is accumulated by $(n+1)$-pulse heteroclinic tangencies for nearby parameter values.*

Due to the negative divergence at both saddle-foci, heteroclinic tangencies give rise to attracting periodic solutions of large periods and small basins of attraction, appearing in large numbers, possibly infinite. For $\lambda \approx 0$, return maps to appropriate domains close to the tangency are conjugate to Hénon-like maps [8, 26]. As $\lambda \to 0$, in V^0, infinitely many wild attractors coexist with suspended horseshoes that are being destroyed.

Theorem 7. *For a family f_λ in the open set $\mathcal{C}$ of Theorem 5, there is a sequence of closed intervals $\Delta_n = [c_n, d_n]$, with $0 < d_{n+1}, c_n < d_n$ and $\lim_{n\to\infty} d_n = 0$, such that as λ decreases in Δ_n, a suspended horseshoe is destroyed.*

A similar result has been formulated by Newhouse [27] and Yorke and Alligood [39] for the case of two dimensional diffeomorphisms in the context of homoclinic bifurcations with no references to the equivariance. A more precise formulation of the result is given in Section 6. Applying the results of [39, 29] to this family, we obtain:

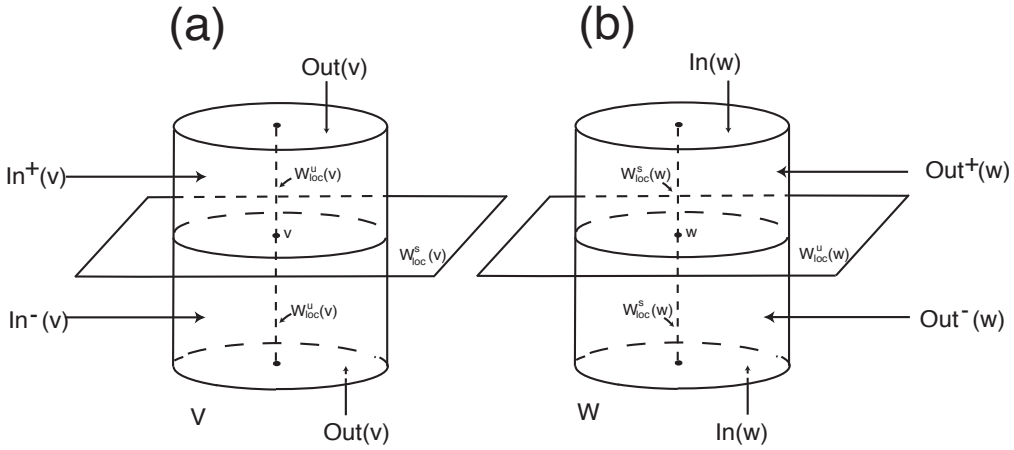

FIGURE 2. Cylindrical neighbourhoods of the saddle-foci $\mathbf{v}$ (a) and $\mathbf{w}$ (b).

Corollary 8. *For a family f_λ in the open set $\mathcal{C}$ of Theorem 5, and λ in one of the intervals Δ_n of Theorem 7 the flow of $\dot{x} = f_\lambda(x)$ undergoes infinitely many saddle-node and period doubling bifurcations.*

With an additional hypothesis we get:

Corollary 9. *For a family f_λ in the open set $\mathcal{C}$ of Theorem 5, if the first return to a transverse section is area-contracting, then for parameters λ in an open subset of Δ_n with sufficiently large n, infinitely many attracting periodic solutions coexist.*

In Section 6 we also describe a setting where the additional hypothesis holds.

When λ decreases, the Cantor set of points of the horseshoes that remain near the cycle is losing topological entropy, as the set loses hyperbolicity, a phenomenon similar to that described in [13].

4. Local geometry and transition maps

We analyse the dynamics near the network by deriving local maps that approximate the dynamics near and between the two nodes in the network. In this section we establish the notation that will be used in the rest of the article and the expressions for the local maps. We start with appropriate coordinates near the two saddle-foci.

4.1. **Local coordinates.** In order to describe the dynamics around the Bykov cycles of Σ^λ, we introduce local coordinates near the equilibria $\mathbf{v}$ and $\mathbf{w}$. By Samovol's Theorem [35], the vector field f_λ is C^1-conjugate to its linear part around each saddle-focus. Without loss of generality we assume that $\alpha_\mathbf{v} = \alpha_\mathbf{w} = 1$. In cylindrical coordinates (ρ, θ, z) the linearisation at $\mathbf{v}$ is given by:

$$\dot{\rho} = -C_\mathbf{v}\rho \qquad \dot{\theta} = 1 \qquad \dot{z} = E_\mathbf{v} z$$

and around $\mathbf{w}$ takes the form:

$$\dot{\rho} = E_\mathbf{w}\rho \qquad \dot{\theta} = 1 \qquad \dot{z} = -C_\mathbf{w} z.$$

In these coordinates, we consider cylindrical neighbourhoods V and W in $\mathbf{S}^3$ of $\mathbf{v}$ and $\mathbf{w}$, respectively, of radius $\rho = \varepsilon > 0$ and height $z = 2\varepsilon$ — see Figure 2. After a linear rescaling of

the variables, we may also assume that $\varepsilon = 1$. Their boundaries consist of three components: the cylinder wall parametrised by $x \in \mathbf{R} \pmod{2\pi}$ and $|y| \leq 1$ with the usual cover

$$(x, y) \mapsto (1, x, y) = (\rho, \theta, z)$$

and two discs, the top and bottom of the cylinder. We take polar coverings of these disks

$$(r, \varphi) \mapsto (r, \varphi, \pm 1) = (\rho, \theta, z)$$

where $0 \leq r \leq 1$ and $\varphi \in \mathbf{R} \pmod{2\pi}$. The local stable manifold of $\mathbf{v}$, $W^s(\mathbf{v})$, corresponds to the circle parametrised by $y = 0$. In V we use the following terminology suggested in Figure 2:

- $In(\mathbf{v})$, the cylinder wall of V, consisting of points that go inside V in positive time;
- $Out(\mathbf{v})$, the top and bottom of V, consisting of points that go outside V in positive time.

We denote by $In^+(\mathbf{v})$ the upper part of the cylinder, parametrised by (x, y), $y \in [0, 1]$ and by $In^-(\mathbf{v})$ its lower part.

The cross sections obtained for the linearisation around $\mathbf{w}$ are dual to these. The set $W^s(\mathbf{w})$ is the z-axis intersecting the top and bottom of the cylinder W at the origin of its coordinates. The set $W^u(\mathbf{w})$ is parametrised by $z = 0$, and we use:

- $In(\mathbf{w})$, the top and bottom of W, consisting of points that go inside W in positive time;
- $Out(\mathbf{w})$, the cylinder wall of W, consisting of points that go inside W in negative time, with $Out^+(\mathbf{w})$ denoting its upper part, parametrised by (x, y), $y \in [0, 1]$ and $Out^-(\mathbf{w})$ its lower part.

We will denote by $W^u_{loc}(\mathbf{w})$ the portion of $W^u(\mathbf{w})$ that goes from $\mathbf{w}$ up to $In(\mathbf{v})$ not intersecting the interior of V and by $W^s_{loc}(\mathbf{v})$ the portion of $W^s(\mathbf{v})$ outside W that goes directly from $Out(\mathbf{w})$ into $\mathbf{v}$.

The flow is transverse to these cross sections and the boundaries of V and of W may be written as the closure of $In(\mathbf{v}) \cup Out(\mathbf{v})$ and $In(\mathbf{w}) \cup Out(\mathbf{w})$, respectively.

4.2. **Transition maps near the saddle-foci.** The trajectory of a point (x, y) with $y > 0$ in $In(\mathbf{v})$, leaves V at $Out(\mathbf{v})$ at

$$\Phi_{\mathbf{v}}(x, y) = \left(y^{\delta_{\mathbf{v}}}, -\frac{\ln y}{E_{\mathbf{v}}} + x \right) = (r, \phi) \qquad \text{where} \qquad \delta_{\mathbf{v}} = \frac{C_{\mathbf{v}}}{E_{\mathbf{v}}} > 1 \ . \tag{4.1}$$

Similarly, a point (r, ϕ) in $In(\mathbf{w}) \backslash W^s(\mathbf{w})$, leaves W at $Out(\mathbf{w})$ at

$$\Phi_{\mathbf{w}}(r, \varphi) = \left(-\frac{\ln r}{E_{\mathbf{w}}} + \varphi, r^{\delta_{\mathbf{w}}} \right) = (x, y) \qquad \text{where} \qquad \delta_{\mathbf{w}} = \frac{C_{\mathbf{w}}}{E_{\mathbf{w}}} > 1 \ . \tag{4.2}$$

4.3. **Transition map along the connection $[\mathbf{v} \to \mathbf{w}]$.** Points in $Out(\mathbf{v})$ near $W^u_{loc}(\mathbf{v})$ are mapped into $In(\mathbf{w})$ in a flow-box along the each one of the connections $[\mathbf{v} \to \mathbf{w}]$. Without loss of generality, we will assume that the transition $\Psi_{\mathbf{v}\to\mathbf{w}} : Out(\mathbf{v}) \to In(\mathbf{w})$ does not depend on λ and is modelled by the identity, which is compatible with hypothesis (P5). Using a more general form for $\Psi_{\mathbf{v}\to\mathbf{w}}$ would complicate the calculations without any change in the final results.

The coordinates on V and W are chosen to have $[\mathbf{v} \to \mathbf{w}]$ connecting points with $z > 0$ in V to points with $z > 0$ in W. We will denote by η the map $\eta = \Phi_{\mathbf{w}} \circ \Psi_{\mathbf{v}\to\mathbf{w}} \circ \Phi_{\mathbf{v}}$. From (4.1) and (4.2), its expression in local coordinates, for $y > 0$, is

$$\eta(x, y) = \left(x - K \ln y, y^{\delta} \right) \qquad \text{with} \qquad \delta = \delta_{\mathbf{v}} \delta_{\mathbf{w}} > 1 \qquad \text{and} \qquad K = \frac{C_{\mathbf{v}} + E_{\mathbf{w}}}{E_{\mathbf{v}} E_{\mathbf{w}}} > 0. \tag{4.3}$$

4.4. **Geometry of the transition map.** Consider a cylinder C parametrised by a covering $(\theta, y) \in \mathbf{R} \times [-1, 1]$, where θ is periodic. A *helix* on the cylinder C *accumulating on the circle* $y = 0$ is a curve on C without self-intersections, that is the image by the covering map of a continuous map $H : (a, b) \to \mathbf{R} \times [-1, 1]$, $H(s) = (H_\theta(s), H_y(s))$, satisfying:

$$\lim_{s\to a^+} H_\theta(s) = \lim_{s\to b^-} H_\theta(s) = \pm\infty, \qquad \lim_{s\to a^+} H_y(s) = \lim_{s\to b^-} H_y(s) = 0$$

and such that there are $\tilde{a} \leq \tilde{b} \in (a, b)$ for which both $H_\theta(s)$ and $H_y(s)$ are monotonic in each of the intervals $(a, \tilde{a})$ and $(\tilde{b}, b)$. It follows from the assumptions on the function H_θ that it has either a global minimum or a global maximum, since $\lim_{s\to a^+} H_\theta(s) = \lim_{s\to b^-} H_\theta(s)$. At the corresponding point, the projection of the helix into the circle $y = 0$ is singular, a *fold point* of the helix. Similarly, the function H_y always has a global maximum, that will be called the *maximum height* of the helix. See Figure 3.

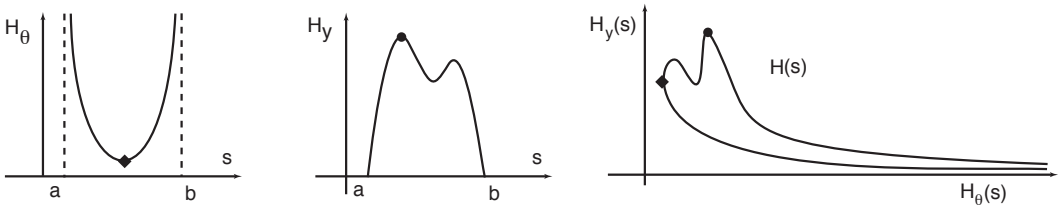

FIGURE 3. A helix is defined on a covering of the cylinder by a smooth curve $(H_\theta(s), H_y(s))$ that turns around the cylinder infinitely many times as its height H_y tends do zero. It always contains a fold point, indicated here by a diamond, and a point of maximum height, shown as a black dot.

Lemma 10. *Consider a curve on one of the cylinder walls $In(\mathbf{v})$ or $Out(\mathbf{w})$, parametrised by the graph of a smooth function $h : [a, b] \to \mathbf{R}$, where $b - a < 2\pi$ with $h(a) = h(b) = 0$, $h'(a) > 0$, $h'(b) < 0$ and $h(x) > 0$ for all $x \in (a, b)$. Let M be the global maximum value of h, attained at a point $x_M \in (a, b)$. Then, for the transition maps defined above, we have:*

1. *if the curve lies in $In(\mathbf{v})$ then it is mapped by $\eta = \Phi_{\mathbf{w}} \circ \Psi_{\mathbf{v}\to\mathbf{w}} \circ \Phi_{\mathbf{v}}$ into a helix on $Out(\mathbf{w})$ accumulating on the circle $Out(\mathbf{w}) \cap W^u_{loc}(\mathbf{w})$, its maximum height is M^δ and it has a fold point at $\eta(x_*, h(x_*))$ for some $x_* \in (a, x_M)$;*
2. *if the curve lies in $Out(\mathbf{w})$ then it is mapped by η^{-1} into a helix on $In(\mathbf{v})$ accumulating on the circle $In(\mathbf{v}) \cap W^s_{loc}(\mathbf{v})$, its maximum height is $M^{1/\delta}$ and it has a fold point at $\eta^{-1}(x_*, h(x_*))$ for some $x_* \in (x_M, b)$.*

Proof. The graph of h defines a curve on $In(\mathbf{v})$ without self-intersections. Since η is the transition map of a differential equation, hence a diffeomorphism, this curve is mapped by η into a curve $H(x) = \eta(x, h(x)) = (H_\theta(x), H_y(x))$ in $Out(\mathbf{w})$ without self-intersections. Using the expression (4.3) for η, we get

$$H(x) = \left(x - K \ln h(x), (h(x))^\delta\right) \qquad \text{and} \qquad H'(x) = \left(1 - \frac{Kh'(x)}{h(x)}, \delta\frac{(h(x))^\delta h'(x)}{h(x)}\right). \tag{4.4}$$

From this expression it is immediate that

$$\lim_{x\to a^+} H_\theta(x) = \lim_{x\to b^-} H_\theta(x) = +\infty \quad \text{and} \quad \lim_{x\to a^+} H_y(x) = \lim_{x\to b^-} H_y(x) = 0.$$

Also,

$$H_y(x_M) = M^\delta \geq (h(x))^\delta = H_y(x)$$

for all $x \in (a,b)$, so the curve lies below the level $y = M^\delta$ in $Out(\mathbf{w})$. Since $h'(b) < 0$, there is an interval $(\tilde{b}, b)$ where $h'(x) < 0$ and hence $H'_\theta(x) > 0$ and $H_y(x) < 0$. Similarly, $h'(x) > 0$ on some interval $(a, \hat{a})$, where $H'_y > 0$. For the sign of $H'_\theta(x)$, note that $Kh'(a) > 0 = h(a)$ and $Kh'(x_M) = 0 < h(x_M)$. Thus, there is a point $x_* \in (a, x_M)$ where $h(x_*) = Kh'(x_*)$, where $H'_\theta(x)$ changes sign, this is a fold point. If x_* is the minimum value of x for which this happens, then locally the helix lies to the right of this point. This proves assertion (1).

The proof of assertion (2) is similar, using the expression

$$\eta^{-1}(x,y) = \left(x + \frac{K}{\delta} \ln y, y^{1/\delta} \right). \tag{4.5}$$

In this case we get $\lim_{x\to a^+} H_\theta(x) = \lim_{x\to b^-} H_\theta(x) = -\infty$ and if x_* is the largest value of x for which the helix has a fold point, then locally the helix lies to the left of $\eta^{-1}(x_*, h(x_*))$. □

Note that if, instead of the graph of a smooth function, we consider continuous and piecewise smooth curve $\alpha(s)$ without self-intersections from $\alpha(0) = (a,0)$ to $\alpha(1) = (b,0)$, we can apply similar arguments to show that both $\eta(\alpha)$ and $\eta^{-1}(\alpha)$ are helices.

4.5. **Geometry of the invariant manifolds.** There is also a well defined transition map

$$\Psi^\lambda_{\mathbf{w}\to\mathbf{v}} : Out(\mathbf{w}) \longrightarrow In(\mathbf{v})$$

that depends on the $\mathbf{Z}_2\langle\gamma_2\rangle$-symmetry breaking parameter λ, where $\Psi^0_{\mathbf{w}\to\mathbf{v}}$ is the identity map. We will denote by R_λ the map $\Psi^\lambda_{\mathbf{w}\to\mathbf{v}} \circ \eta$, where well defined. When there is no risk of ambiguity, we omit the subscript λ.

In this section we investigate the effect of $\Psi^\lambda_{\mathbf{w}\to\mathbf{v}}$ on the two-dimensional invariant manifolds of $\mathbf{v}$ and $\mathbf{w}$ for $\lambda \neq 0$, under the assumption (P7).

For this, let f_λ be an unfolding of f_0 satisfying (P1)–(P6) and lying in the C^2-open set $\mathcal{C}_1$ of unfoldings that satisfy (P7). For $\lambda \neq 0$, we introduce the notation, see Figure 4:

- $(P^1_{\mathbf{w}}, 0)$ and $(P^2_{\mathbf{w}}, 0)$ with $0 < P^1_{\mathbf{w}} < P^2_{\mathbf{w}} < 2\pi$ are the coordinates of the two points where the connections $[\mathbf{w} \to \mathbf{v}]$ of Property (P7) meet $Out(\mathbf{w})$;
- $(P^1_{\mathbf{v}}, 0)$ and $(P^2_{\mathbf{v}}, 0)$ with $0 < P^1_{\mathbf{v}} < P^2_{\mathbf{v}} < 2\pi$ are the coordinates of the two points where $[\mathbf{w} \to \mathbf{v}]$ meets $In(\mathbf{v})$;
- $(P^j_{\mathbf{w}}, 0)$ and $(P^j_{\mathbf{v}}, 0)$ are on the same trajectory for each $j = 1, 2$.

By (P7), the manifolds $W^u_{loc}(\mathbf{w})$ and $W^s_{loc}(\mathbf{v})$ intersect transversely for $\lambda \neq 0$. For λ close to zero, we are assuming that $W^s_{loc}(\mathbf{v})$ intersects the wall $Out(\mathbf{w})$ of the cylinder W on a closed curve as in Figure 4. It corresponds to the expected unfolding from the coincidence of the manifolds $W^s(\mathbf{v})$ and $W^u(\mathbf{w})$ at f_0. Similarly, $W^u_{loc}(\mathbf{w})$ intersects the wall $In(\mathbf{v})$ of the cylinder V on a closed curve. For small $\lambda > 0$, these curves can be seen as graphs of smooth 2π-periodic functions, for which we make the following conventions:

- $W^s_{loc}(\mathbf{v}) \cap Out(\mathbf{w})$ is the graph of $y = h_{\mathbf{v}}(x, \lambda)$, with $h_{\mathbf{v}}(P^j_{\mathbf{w}}, \lambda) = 0$, $j = 1, 2$;
- $W^u_{loc}(\mathbf{w}) \cap In(\mathbf{v})$ is the graph of $y = h_{\mathbf{w}}(x, \lambda)$, with $h_{\mathbf{w}}(P^j_{\mathbf{v}}, \lambda) = 0$, $j = 1, 2$;
- $h_{\mathbf{v}}(x, 0) \equiv 0$ and $h_{\mathbf{w}}(x, 0) \equiv 0$
- for $\lambda > 0$, we have $h'_{\mathbf{v}}(P^1_{\mathbf{w}}, \lambda) > 0$, hence $h'_{\mathbf{v}}(P^2_{\mathbf{w}}, \lambda) < 0$ and $h'_{\mathbf{w}}(P^1_{\mathbf{v}}, \lambda) < 0, h'_{\mathbf{w}}(P^2_{\mathbf{v}}, \lambda) > 0$.

The two points $(P^1_{\mathbf{w}}, 0)$ and $(P^2_{\mathbf{w}}, 0)$ divide the closed curve $y = h_{\mathbf{v}}(x, \lambda)$ in two components, corresponding to different signs of the second coordinate. With the conventions above, we get $h_{\mathbf{v}}(x, \lambda) > 0$ for $x \in \left(P^1_{\mathbf{w}}, P^2_{\mathbf{w}}\right)$. Then the region W^- in $Out(\mathbf{w})$ delimited by $W^s_{loc}(\mathbf{v})$ and

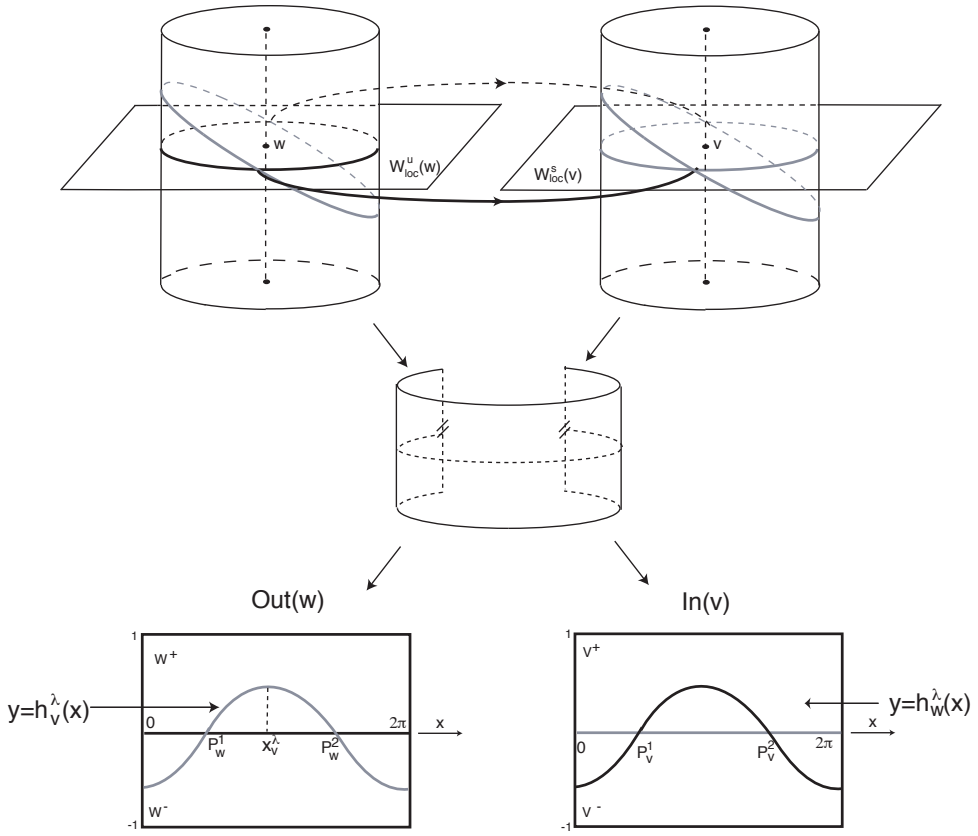

FIGURE 4. For λ close to zero, $W^s(\mathbf{v})$ intersects the wall $Out(\mathbf{w})$ of the cylinder W on a closed curve, given in local coordinates as the graph of a periodic function. Similarly, $W^u(\mathbf{w})$ meets $In(\mathbf{v})$ on a closed curve — this is the expected unfolding from the coincidence of the invariant manifolds at $\lambda = 0$.

$W^u_{loc}(\mathbf{w})$ between $P^1_\mathbf{w}$ and $P^2_\mathbf{w}$ gets mapped by $\Psi^\lambda_{\mathbf{w}\to\mathbf{v}}$ into $In^-(\mathbf{v})$, while all other points in $Out^+(\mathbf{w})$ are mapped into $In^+(\mathbf{v})$. We denote by W^+ the latter set, of points in $Out(\mathbf{w})$ with $0 < y < 1$ and $y > h_\mathbf{w}(x,\lambda)$ for $x \in \left(P^1_\mathbf{w}, P^2_\mathbf{w}\right)$. The maximum value of $h_\mathbf{v}(x,\lambda)$ is attained at some point

$$(x,y) = (x_\mathbf{v}(\lambda), M_\mathbf{v}(\lambda)) \qquad \text{with} \qquad P^1_\mathbf{w} < x_\mathbf{v}(\lambda) < P^2_\mathbf{w}.$$

Finally, let $M_\mathbf{w}(\lambda)$ be the maximum of $h_\mathbf{w}(x,\lambda)$, attained at a point $x_\mathbf{w}(\lambda) \in \left(P^2_\mathbf{v}, P^1_\mathbf{v}\right)$. With this notation, we have:

Proposition 11. *Let f_λ be family of vector fields satisfying (P1)–(P7). For $\lambda \neq 0$ sufficiently small, the portion of $W^u_{loc}(\mathbf{w}) \cap In(\mathbf{v})$ that lies in $In^+(\mathbf{v})$ is mapped by η into a helix in $Out(\mathbf{w})$ accumulating on $W^u_{loc}(\mathbf{w})$. If $M_\mathbf{w}(\lambda)$ is the maximum height of $W^u_{loc}(\mathbf{w}) \cap In^+(\mathbf{v})$, then the maximum height of the helix is $M_\mathbf{w}(\lambda)^\delta$. For each $\lambda > 0$ there is a fold point in the helix that, as λ tends to zero, turns around the cylinder $Out(\mathbf{w})$ infinitely many times.*

Proof. That η maps $W^u_{loc}(\mathbf{w}) \cap In^+(\mathbf{v})$ into a helix, and the statement about its maximum height follow directly by applying assertion (1) of Lemma 10 to $h_\mathbf{w}$. For the fold point in the helix, let

$x_*(\lambda)$ be its first coordinate. From the expression (4.3) of η it follows that

$$x_*(\lambda) = x_\lambda - K \ln h_{\mathbf{w}}(x_\lambda)$$

for some $x_\lambda \in (P^1_{\mathbf{w}}, x_{\mathbf{v}}(\lambda))$ and with $h_{\mathbf{w}}(x_\lambda) \leq h_{\mathbf{w}}(x_{\mathbf{v}}(\lambda), \lambda) = M_{\mathbf{v}}(\lambda)$ and hence,

$$-K \ln h_{\mathbf{w}}(x_\lambda, \lambda) \geq -K \ln M_{\mathbf{v}}(\lambda).$$

Since f_λ unfolds f_0, then $\lim_{\lambda\to 0} M_{\mathbf{v}}(\lambda) = 0$, hence $\lim_{\lambda\to 0} -K \ln h_{\mathbf{w}}(x_\lambda, \lambda) = \infty$ and therefore, the fold point turns around the cylinder $Out(\mathbf{w})$ infinitely many times. □

5. Heteroclinic Tangencies

Using the notation and results of Section 4 we can now discuss the tangencies of the invariant manifolds and prove Theorems 5 and 6. As remarked in Section 4.5, since f_λ unfolds f_0, then the maximum heights, $M_{\mathbf{v}}(\lambda)$ of $W^s_{loc}(\mathbf{v}) \cap Out(\mathbf{w})$, and $M_{\mathbf{w}}(\lambda)$ of $W^u_{loc}(\mathbf{w}) \cap In(\mathbf{v})$, satisfy:

$$\lim_{\lambda\to 0} M_{\mathbf{v}}(\lambda) = \lim_{\lambda\to 0} M_{\mathbf{w}}(\lambda) = 0.$$

We make the additional assumption that $(M_{\mathbf{w}}(\lambda))^\delta$ tends to zero faster than $M_{\mathbf{v}}(\lambda)$. This condition defines the open set $\mathcal{C} \subset \mathcal{C}_1$ of unfoldings f_λ that we need for the statement of Theorem 5. More precisely, let $\mathcal{C}$ be the set of unfoldings of f_0 that satisfy (P7) and for which there is a value $\lambda_* > 0$ such that for $0 < \lambda < \lambda_*$ we have $(M_{\mathbf{w}}(\lambda))^\delta < M_{\mathbf{v}}(\lambda)$. Then $\mathcal{C}$ is open in the C^2 topology.

Proof of Theorem 5. Suppose $f_\lambda \in \mathcal{C}$. By Proposition 11, the curve

$$\alpha^\lambda(x) = \eta\left(x, h_{\mathbf{w}}(x,\lambda), \lambda\right) = \left(\alpha^\lambda_1(x), \alpha^\lambda_2(x)\right), \qquad x \in \left(P^2_{\mathbf{v}}, P^1_{\mathbf{v}}\right) \pmod{2\pi}$$

is a helix in $Out^+(\mathbf{w})$ and has at least one fold point at $x = x_*(\lambda)$. The second coordinate of the helix satisfies $0 < \alpha^\lambda_2(x) < M_{\mathbf{w}}(\lambda)^\delta$ for all $x \in \left(P^2_{\mathbf{v}}, P^1_{\mathbf{v}}\right) \pmod{2\pi}$ and all positive $\lambda < \lambda_*$. Since $f_\lambda \in \mathcal{C}$, then $\alpha^\lambda_2(x) < M_{\mathbf{v}}(\lambda)$ for all x and all positive $\lambda < \lambda_*$.

Moreover, since the fold point $\alpha(x_*(\lambda))$ turns around $Out(\mathbf{w})$ infinitely many times as λ goes to zero, given any $\lambda_0 < \lambda_*$ there exists a positive value $\lambda_R < \lambda_0$ such that $\alpha(x_*(\lambda_R))$ lies in W^+, the region in $Out(\mathbf{w})$ between $W^s_{loc}(\mathbf{v})$ and $W^u_{loc}(\mathbf{w})$ that gets mapped into the upper part of $In(\mathbf{v})$. Since the second coordinate of the fold point is less than the maximum of $h_{\mathbf{v}}$, there is a positive value $\lambda_L < \lambda_R$ such that $\alpha(x_*(\lambda_L))$ lies in W^-, the region in $Out(\mathbf{w})$ that gets mapped into the lower part of $In(\mathbf{v})$, whose boundary contains the graph of $h_{\mathbf{v}}$. Therefore, the curve $\alpha(x_*(\lambda))$ is tangent to the graph of $h_{\mathbf{v}}(x,\lambda)$ at some point $\alpha(x_*(\lambda_1))$ with $\lambda_1 \in (\lambda_L, \lambda_R)$.

We have thus shown that given $\lambda_0 > 0$, there is some positive $\lambda_1 < \lambda_0$, for which the image of the curve $W^u_{loc}(\mathbf{w}) \cap In(\mathbf{v})$ by η is tangent to $W^s_{loc}(\mathbf{v}) \cap Out(\mathbf{w})$, creating a 1-pulse heteroclinic tangency. Two transverse 1-pulse heteroclinic connections exist for $\lambda > \lambda_1$ close to λ_1. These connections come together at the tangency and disappear.

As λ goes to zero, the fold point $\alpha(x_*(\lambda))$ turns around the cylinder $Out(\mathbf{w})$ infinitely many times, thus going in and out of W^-. Each times it crosses the boundary, a new tangency occurs. Repeating the argument above yields the sequence λ_i of parameter values for which there is a 1-pulse heteroclinic tangency and this completes the proof of the main statement of Theorem 5.

On the other hand, as λ goes to zero, the maximum height of the helix, $(M_{\mathbf{w}}(\lambda))^\delta$ also tends to zero. This implies that the second coordinate of the points $\alpha(x_*(\lambda_i)) \in Out(\mathbf{w})$ where there is a 1-pulse heteroclinic tangency tends to zero as i goes to infinity. This shows that the tangency approaches the two-dimensional $[\mathbf{w} \to \mathbf{v}]$ connection that exists for $\lambda = 0$. □

The construction in the proof of Theorem 5 may be extended to obtain multipulse tangencies, as follows:

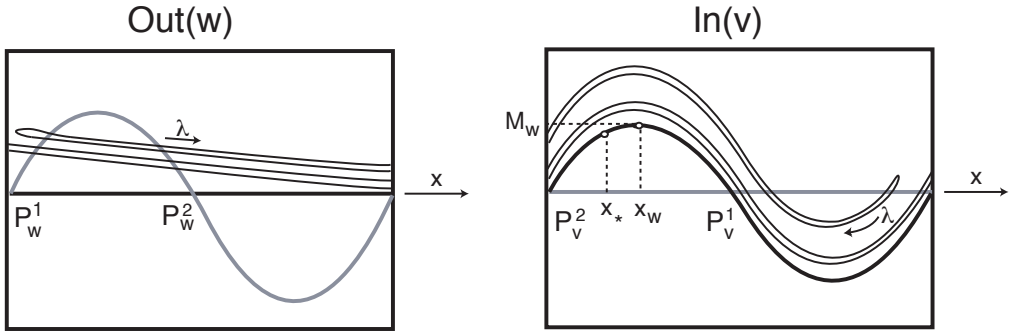

FIGURE 5. Left: when λ decreases, the fold point of the helix $\alpha(x) \in Out(\mathbf{w})$ moves to the right and for $\lambda = \lambda_i$ it is tangent to $W^s_{loc}(\mathbf{v})$ creating a 1-pulse tangency. Right: $\Psi_{[\mathbf{w}\to\mathbf{v}]}$ maps the helix $\alpha(x)$ close to $W^u_{loc}(\mathbf{w}) \cap In(\mathbf{v})$, creating several curves that satisfy the hypotheses of Lemma 10 (1). These curves are again mapped by η into helices in $Out(\mathbf{w})$ creating 2-pulse heteroclinic tangencies.

Proof of Theorem 6. Look at $W^u_{loc}(\mathbf{w}) \cap In(\mathbf{v})$, the graph of $h_{\mathbf{w}}(x, \lambda)$. Since $h'_{\mathbf{w}}(P^1_{\mathbf{v}}, \lambda) < 0$, there is an interval $[\tilde{x}, P^1_{\mathbf{v}}] \subset [x_{\mathbf{w}}, P^1_{\mathbf{v}}]$ where the map $h_{\mathbf{w}}$ is monotonically decreasing. Therefore, we may define infinitely many intervals where $\alpha^\lambda(x) = \eta\,(x, h_{\mathbf{w}}(x, \lambda))$ lies in W^+. More precisely, we have two sequences, (a_j) and (b_j) in $[\tilde{x}, P^1_{\mathbf{v}}]$ such that:

- $a_j < b_j < a_{j+1}$ with $\lim_{j\to\infty} a_j = P^1_{\mathbf{v}}$;
- $\alpha(a_j)$ and $\alpha(b_j) \in W^s_{loc}(\mathbf{v}) \cap Out^+(\mathbf{w})$;
- if $x \in (a_j, b_j)$ then $\alpha(x) \in W^+$;
- the curves $\alpha\,([a_j, b_j])$ accumulate uniformly on $W^u_{loc}(\mathbf{w}) \cap Out(\mathbf{w})$ as $j \to \infty$.

Hence, each one of the curves $\alpha\,([a_j, b_j])$ is mapped by $\Psi_{\mathbf{w}\to\mathbf{v}}$ into the graph of a function h in $In(\mathbf{v})$ satisfying the conditions of Lemma 10, and hence each one of these curves is mapped by η into a helix $\xi_j(x)$, $x \in (a_j, b_j)$.

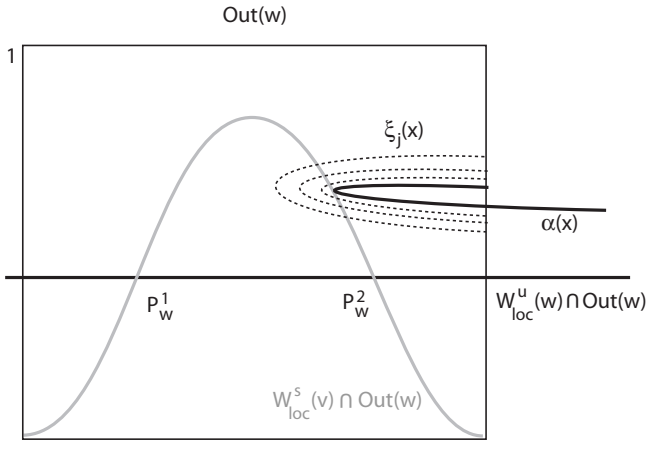

FIGURE 6. Curves in the proof of Theorem 6: for $\lambda = \lambda_i$ the curve $\alpha(x) = \eta(W^u_{loc}(\mathbf{w}) \cap In(\mathbf{v}))$ (solid black curve) is tangent to $W^s_{loc}(\mathbf{v})$ (gray curve) in $Out(\mathbf{w})$. The curves $\xi_j(x)$ (dotted) accumulate on $\alpha(x)$. Very small changes in λ make them tangent to $W^s_{loc}(\mathbf{v})$ creating 2-pulse heteroclinic tangencies.

Let λ_i be a parameter value for which $\dot{x} = f_{\lambda_i}(x)$ has a 1-pulse heteroclinic tangency as stated in Theorem 5. As $j \to +\infty$, the helices $\xi_j(x)$ accumulate on the helix of Theorem 5 as drawn in Figure 6, hence the fold point of $\xi_j(x)$ is arbitrarily close to the fold point of $\eta(x, h_{\mathbf{w}}(x, \lambda))$. The arguments in the proof of Theorem 5 show that a small change in the parameter λ makes the new helix tangent to $W^s_{loc}(\mathbf{v})$ as in Figure 5. For each j this creates a 2-pulse heteroclinic tangency at $\lambda = \lambda_{ij}$. Since the the helices $\xi_j(x)$ accumulate on $\alpha^{\lambda_i}(x)$, it follows that $\lim_{j\in\mathbf{N}} \lambda_{ij} = \lambda_i$.

Finally, the argument may be applied recursively to show that each n-pulse heteroclinic tangency is accumulated by $(n+1)$-pulse heteroclinic tangencies for nearby parameter values. □

If $\lambda^\star \in \mathbf{R}$ is such that the flow of $\dot{x} = f_{\lambda^\star}(x)$ has a heteroclinic tangency, when λ varies near $\lambda^\star$, we find the creation and the destruction of horseshoes that is accompanied by Newhouse phenomena [13, 39]. In terms of numerics, we know very little about the geometry of these attractors, we also do not know the size and the shape of their basins of attraction.

6. Bifurcating dynamics

We discuss here the geometric constructions that determine the global dynamics near a Bykov cycle, in order to prove Theorem 7. For this we need some preliminary definitions and more information on the geometry of the transition maps. First, we adapt the definition of horizontal strip in [15] to serve our purposes: for $\tau > 0$ sufficiently small, in the local coordinates of the walls of the cylinders V and W, consider the rectangles:

$$\mathcal{S}_{\mathbf{v}} = [P^2_{\mathbf{v}} - \tau, P^1_{\mathbf{v}} + \tau] \times [0, 1] \subset In(\mathbf{v}) \qquad \text{and} \qquad \mathcal{S}_{\mathbf{w}} = [P^2_{\mathbf{w}} - \tau, P^1_{\mathbf{w}} + \tau] \times [0, 1] \subset Out(\mathbf{w})$$

with the conventions $-\pi < P^2_{\mathbf{v}} - \tau < P^1_{\mathbf{v}} + \tau \leq \pi$ and $-\pi < P^2_{\mathbf{w}} - \tau < P^1_{\mathbf{w}} + \tau \leq \pi$.

A *horizontal strip* in $\mathcal{S}_{\mathbf{v}}$ is a subset of $In^+(\mathbf{v})$ of the form

$$\mathcal{H} = \left\{(x, y) \in In^+(\mathbf{v}) : \quad x \in [P^2_{\mathbf{v}} - \tau, P^1_{\mathbf{v}} + \tau] \qquad \text{and} \quad y \in [u_1(x), u_2(x)]\right\},$$

where $u_1, u_2 : [P^2_{\mathbf{v}} - \tau, P^1_{\mathbf{v}} + \tau] \to (0, 1]$ are smooth maps such that $u_1(x) < u_2(x)$ for all $x \in [P^2_{\mathbf{v}} - \tau, P^1_{\mathbf{v}} + \tau]$. The graphs of the u_j are called the *horizontal boundaries* of $\mathcal{H}$ and the segments $\big(P^2_{\mathbf{v}} - \tau, y\big)$, $u_1(P^2_{\mathbf{v}} - \tau) \leq y \leq u_2(P^2_{\mathbf{v}} - \tau)$ and $\big(P^1_{\mathbf{v}} + \tau, y\big)$, with $u_1(P^1_{\mathbf{v}} + \tau) \leq y \leq u_2(P^1_{\mathbf{v}} + \tau)$ are its *vertical boundaries*. Horizontal and vertical boundaries intersect at four *vertices*. The *maximum height* and the *minimum height* of $\mathcal{H}$ are, respectively

$$\max_{x\in[P^2_{\mathbf{v}}-\tau, P^1_{\mathbf{v}}+\tau]} u_2(x) \qquad\qquad \min_{x\in[P^2_{\mathbf{v}}-\tau, P^1_{\mathbf{v}}+\tau]} u_1(x).$$

Analogously we may define a *horizontal strip* in $\mathcal{S}_{\mathbf{w}} \subset Out^+(\mathbf{w})$.

A *horseshoe strip* in $\mathcal{S}_{\mathbf{v}}$ is a subset of $In^+(\mathbf{v})$ of the form

$$\left\{(x, y) \in In^+(\mathbf{v}) : \quad x \in [a_2, b_2], \quad y \in [u_1(x), u_2(x)]\right\},$$

where

- $[a_1, b_1] \subset [a_2, b_2] \subset [P^2_{\mathbf{v}} - \tau, P^1_{\mathbf{v}} + \tau]$;
- $u_1(a_1) = u_1(b_1) = 0$;
- $u_2(a_2) = u_2(b_2) = 0$.

The boundary of $\mathcal{H}$ consists of the graph of $u_2(x)$, $x \in [a_2, b_2]$, the graph of $u_1(x)$, $x \in [a_1, b_1]$, together with the two pieces of $W^s_{loc}(\mathbf{v}) \cap In(\mathbf{v})$ with $x \in [a_2, a_1]$ and $x \in [b_1, b_2]$.

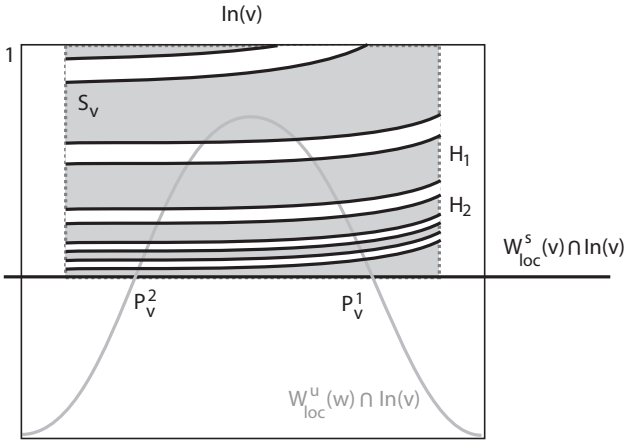

FIGURE 7. For $\lambda > 0$ sufficiently small, the set $\eta^{-1}(\mathcal{S}_{\mathbf{w}}) \cap \mathcal{S}_{\mathbf{v}}$ has infinitely many connected components (gray area), all of which, except maybe for the top ones, define horizontal strips in $\mathcal{S}_{\mathbf{v}}$ accumulating on $W^s_{loc}(\mathbf{v}) \cap In(\mathbf{v})$ (gray curve).

6.1. **Horseshoe strips in $\mathcal{S}_{\mathbf{v}}$.** We are interested in the dynamics of points whose trajectories start in $\mathcal{S}_{\mathbf{v}}$ and return to $In^+(\mathbf{v})$ arriving at $\mathcal{S}_{\mathbf{v}}$.

Lemma 12. *The set $\eta^{-1}(\mathcal{S}_{\mathbf{w}}) \cap \mathcal{S}_{\mathbf{v}}$ has infinitely many connected components all of which are horizontal strips in $\mathcal{S}_{\mathbf{v}}$ accumulating on $W^s_{loc}(\mathbf{v}) \cap In(\mathbf{v})$, except maybe for a finite number. The horizontal boundaries of these strips are graphs of monotonically increasing functions of x.*

Proof. The boundary of $\mathcal{S}_{\mathbf{w}}$ consists of the following:

(1) a piece of $W^u_{loc}(\mathbf{w}) \cap Out(\mathbf{w})$ parametrised by $y = 0$, $x \in [P^1_{\mathbf{w}} - \tau, P^2_{\mathbf{w}} + \tau]$, where η^{-1} is not defined;
(2) the horizontal segment $(x, 1)$ with $x \in [P^2_{\mathbf{w}} - \tau, P^1_{\mathbf{w}} + \tau]$;
(3) two vertical segments $\left(P^1_{\mathbf{w}} - \tau, y\right)$ and $\left(P^2_{\mathbf{w}} + \tau, y\right)$ with $y \in (0, 1)$.

Together, the components (2) and (3) form a continuous curve that, by the arguments of Lemma 10 (2), is mapped by η into a helix on $In^+(\mathbf{v})$, accumulating on $W^s_{loc}(\mathbf{v}) \cap In(\mathbf{v})$. As the helix approaches $W^s_{loc}(\mathbf{v})$, it crosses the vertical boundaries of $\mathcal{S}_{\mathbf{v}}$ infinitely many times. The interior of $\mathcal{S}_{\mathbf{w}}$ is mapped into the space between consecutive crossings, intersecting $\mathcal{S}_{\mathbf{v}}$ in horizontal strips, as shown in Figure 7. From the expression (4.5) of η^{-1} it also follows that the vertical boundaries of $\mathcal{S}_{\mathbf{w}}$ are mapped into graphs of monotonically increasing functions of x. □

Denote by $\mathcal{H}_n$ the strip that attains its maximum height h_n at the vertex $\left(P^1_{\mathbf{v}} + \tau, h_n\right)$ with

$$h_n = \mathrm{e}^{(P^1_{\mathbf{v}} - P^2_{\mathbf{w}} + 2\tau - 2n\pi)/K}, \tag{6.6}$$

then $\lim_{n\to\infty} h_n = 0$, hence the strips $\mathcal{H}_n$ accumulate on $W^s_{loc}(\mathbf{v}) \cap In(\mathbf{v})$. The minimum height of $\mathcal{H}_n$ is given by

$$m_n = \mathrm{e}^{(P^2_{\mathbf{v}} - P^1_{\mathbf{w}} - 2\tau - 2n\pi)/K} \tag{6.7}$$

and is attained at the vertex $\left(P^2_{\mathbf{v}} - \tau, m_n\right)$. Moreover $n < m$ implies that $\mathcal{H}_n$ lies above $\mathcal{H}_m$.

Lemma 13. *Let $\mathcal{H}_n$ be one of the horizontal strips in $\eta^{-1}(\mathcal{S}_{\mathbf{w}}) \cap \mathcal{S}_{\mathbf{v}}$. Then $\eta(\mathcal{H}_n)$ is a horizontal strip in $\mathcal{S}_{\mathbf{w}}$. The strips $\eta(\mathcal{H}_n)$ accumulate on $W^u_{loc}(\mathbf{w}) \cap In(\mathbf{v})$ as $n \to \infty$ and the maximum height of $\eta(\mathcal{H}_n)$ is h_n^δ, where h_n is the maximum height of $\mathcal{H}_n$.*

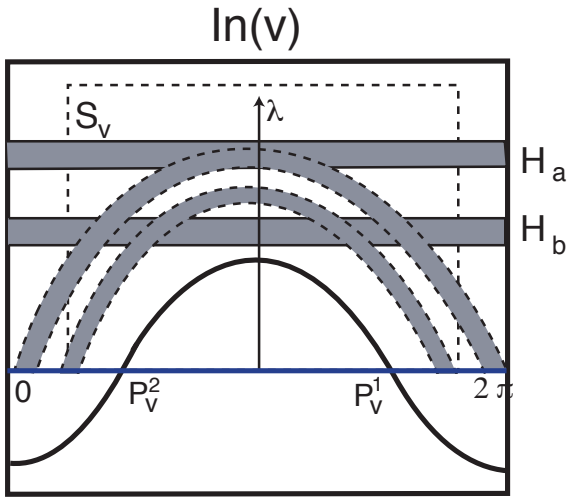

FIGURE 8. Horseshoe strips: for $\lambda > 0$ sufficiently small, the set $R_\lambda(\eta^{-1}(\mathcal{S}_\mathbf{w}) \cap \mathcal{S}_\mathbf{v}) \subset In^+(\mathbf{v})$ defines a countably infinite number of horseshoe strips in $\mathcal{S}_\mathbf{v}$, that accumulate on $W^u_{loc}(\mathbf{w}) \cap In(\mathbf{v})$.

Proof. The boundary of $\mathcal{S}_\mathbf{v}$ consists of a piece of $W^s_{loc}(\mathbf{v})$ plus a curve formed by three segments, two of which are vertical and a horizontal one. From the arguments of Lemma 10 (1), it follows that the part of the boundary of $\mathcal{S}_\mathbf{v}$ not contained in $W^s_{loc}(\mathbf{v})$ is mapped by η into a helix.

Consider now the effect of η on the boundary of $\mathcal{H}_n$. Each horizontal boundary gets mapped into a piece of one of the vertical boundaries of $\mathcal{S}_\mathbf{w}$. The vertical boundaries of $\mathcal{H}_n$ are contained in those of $\mathcal{S}_\mathbf{v}$ and hence are mapped into two pieces of a helix, that will form the horizontal boundaries of the strip $\eta(\mathcal{H}_n)$, that may be written as graphs of decreasing functions of x.

A shown after Lemma 12, the maximum height of $\mathcal{H}_n$ tends to zero, hence the strips $\eta(\mathcal{H}_n)$ have the same property. The maximum height of $\eta(\mathcal{H}_n)$ is h^δ_n, attained at the point $\left(P^2_\mathbf{w} - \tau, h^\delta_n\right)$. □

Lemma 14. *For each $\lambda > 0$ sufficiently small, there exists $n_0(\lambda)$ such that for all $n \geq n_0$ the image $R_\lambda(\mathcal{H}_n)$ of the horizontal strips in $\eta^{-1}(\mathcal{S}_\mathbf{w}) \cap \mathcal{S}_\mathbf{v}$ intersects $\mathcal{S}_\mathbf{v}$ in a horseshoe strip. The strips $R_\lambda(\mathcal{H}_n)$ accumulate on $W^u_{loc}(\mathbf{w}) \cap In(\mathbf{v})$ and, when $n \to \infty$, their maximum height tends to $M_\mathbf{w}(\lambda)$, the maximum height of $W^u_{loc}(\mathbf{w}) \cap In(\mathbf{v})$.*

Proof. The curve $W^s_{loc}(\mathbf{v}) \cap Out(\mathbf{w})$ is the graph of the function $h_\mathbf{v}(x, \lambda)$ that is positive for x outside the interval $[P^2_\mathbf{w}, P^1_\mathbf{w}]$ (mod 2π). In particular, $h_\mathbf{v}(P^2_\mathbf{w} - \tau, \lambda) > 0$ and $h_\mathbf{v}(P^2_\mathbf{w} + \tau, \lambda) > 0$ for small $\tau > 0$. Therefore there is a piece of the vertical boundary of $\mathcal{S}_\mathbf{w}$ that lies below $W^s_{loc}(\mathbf{v}) \cap Out(\mathbf{w})$, consisting of the two segments $(P^2_\mathbf{w} - \tau, y)$ with $0 < y < h_\mathbf{v}(P^2_\mathbf{w} - \tau, \lambda)$ and $(P^1_\mathbf{w} + \tau, y)$ with $0 < y < h_\mathbf{v}(P^1_\mathbf{w} + \tau, \lambda)$. For small $\lambda > 0$, these segments are mapped by $\Psi^\lambda_{\mathbf{w}\to\mathbf{v}}$ inside $In^-(\mathbf{v})$.

Let n_0 be such that the maximum height of $\eta(\mathcal{H}_{n_0})$ is less than the minimum of $h_\mathbf{v}(P^2_\mathbf{w} - \tau, \lambda) > 0$ and $h_\mathbf{v}(P^2_\mathbf{w} + \tau, \lambda) > 0$. Then for any $n \geq n_0$ the vertical sides of $\eta(\mathcal{H}_n)$ are mapped by $\Psi^\lambda_{\mathbf{w}\to\mathbf{v}}$ inside $In^-(\mathbf{v})$.

The horizontal boundaries of $\eta(\mathcal{H}_n)$ go across $\mathcal{S}_\mathbf{w}$, so writing them them as graphs of $u_1(x) < u_2(x)$, there is an interval where the second coordinate of $\Psi^\lambda_{\mathbf{w}\to\mathbf{v}}(x, u_j(x))$ is more than $M_\mathbf{w}(\lambda) >$

0, the maximum height of $W^u_{loc}(\mathbf{w}) \cap In^+(\mathbf{v})$. Since the second coordinate of $\Psi^\lambda_{\mathbf{w}\to\mathbf{v}}(x, u_j(x))$ changes sign twice, then it equals zero at two points, hence $R_\lambda(\mathcal{H}_n) \cap \mathcal{S}_\mathbf{v}$ is a horseshoe strip.

We have shown that the maximum height of $\eta(\mathcal{H}_n)$ tends to zero as $n \to \infty$, hence the maximum height of $R_\lambda(\mathcal{H}_n) = \Psi^\lambda_{\mathbf{w}\to\mathbf{v}}(\eta(\mathcal{H}_n))$ tends to $M_\mathbf{w}(\lambda)$. □

6.2. **Regular Intersections of Strips.** We now discuss the global dynamics near the Bykov cycle. The structure of the non-wandering set near the network depends on the geometric properties of the intersection of $\mathcal{H}_n$ and $R_\lambda(\mathcal{H}_n)$.

Let A be a horseshoe strip and B be a horizontal strip in $\mathcal{S}_\mathbf{v}$. We say that A and B *intersect regularly* if $A \cap B \neq \emptyset$ and each one of the horizontal boundaries of A goes across each one of the horizontal boundaries of B. Intersections that are neither empty nor regular, will be called *irregular*.

If the horseshoe strip A and the horizontal strip B intersect regularly, then $A \cap B$ has at least two connected components, see Figure 8. In this and the next subsection, we will find that the horizontal strips $\mathcal{H}_n$ across $\mathcal{S}_\mathbf{v}$ may intersect $R_\lambda(\mathcal{H}_m)$ in the three ways: empty, regular and irregular, but there is an ordering for the type of intersection, as shown in Figure 9.

Lemma 15. *For any given fixed $\lambda > 0$ sufficiently small, there exists $N(\lambda) \in \mathbf{N}$ such that for all $m, n > N(\lambda)$, the horseshoe strips $R_\lambda(\mathcal{H}_m)$ in $\mathcal{S}_\mathbf{v}$ intersect each one of the horizontal strips $\mathcal{H}_n$ regularly.*

Proof. From Lemma 14 we obtain $n_0(\lambda)$ such that all $R_\lambda(\mathcal{H}_m)$ with $m \geq n_0(\lambda)$ are horseshoe strips and their lower horizontal boundary has maximum height bigger than the maximum height $M_\mathbf{w}(\lambda)$ of $W^u_{loc}(\mathbf{w}) \cap In(\mathbf{v})$.

On the other hand, since the strips $\mathcal{H}_n$ accumulate uniformly on $W^s_{loc}(\mathbf{v}) \cap In(\mathbf{v})$, with their maximum height h_n tending to zero, then there exists $n_1(\lambda)$ such that $h_n < M_\mathbf{w}(\lambda)$ for all $n \geq n_1(\lambda)$. Note that the h_n do not depend on λ. Therefore, for $m, n > N(\lambda) = \max\{n_0(\lambda), n_1(\lambda)\}$ both horizontal boundaries of $R_\lambda(\mathcal{H}_m)$ go across the two horizontal boundaries of $\mathcal{H}_n$. □

The constructions of this section also hold for the backwards return map R^{-1} with analogues to Lemmas 12, 13, 14 and 15.

Generically, for $n > N(\lambda)$ each horizontal strip $\mathcal{H}_n$ intersects $R_\lambda(\mathcal{H}_n)$ in two connected components. Thus the dynamics of points whose trajectories always return to $In(\mathbf{v})$ in $\mathcal{H}_n$ may be coded by a full shift on two symbols, that describe which component is visited by the trajectory on each return to $\mathcal{H}_n$. Similarly, trajectories that return to $\mathcal{S}_\mathbf{v}$ inside $\mathcal{H}_n \cup \cdots \cup \mathcal{H}_{n+k}$ may be coded by a full shift on $2k$ symbols. As $k \to \infty$, the strips $\mathcal{H}_{n+k}$ approach $W^s_{loc}(\mathbf{v}) \cap In(\mathbf{v})$ and the number of symbols tends to infinity. We have recovered the horseshoe dynamics described in assertion (5) of Theorem 3.

The regular intersection of Lemma 15 implies the existence of an R_λ-invariant subset in $\eta^{-1}(\mathcal{S}_\mathbf{w}) \cap \mathcal{S}_\mathbf{v}$, the Cantor set of initial conditions:

$$\Lambda = \bigcap_{j\in\mathbf{Z}} \bigcup_{m,n\geq N(\lambda)} \left(R_\lambda{}^j(\mathcal{H}_m) \cap \mathcal{H}_n\right),$$

where the return map to $\eta^{-1}(\mathcal{S}_\mathbf{w}) \cap \mathcal{S}_\mathbf{v}$ is well defined in forward and backward time, for arbitrarily large times. We have shown here that the map R_λ restricted to this set is semi-conjugate to a full shift over a countable alphabet. Results of [2, 21] show that the first return map is hyperbolic in each horizontal strip, implying the full conjugacy to a shift. The set Λ depends strongly on the parameter λ, in the next subsection we discuss its bifurcations when λ decreases to zero.

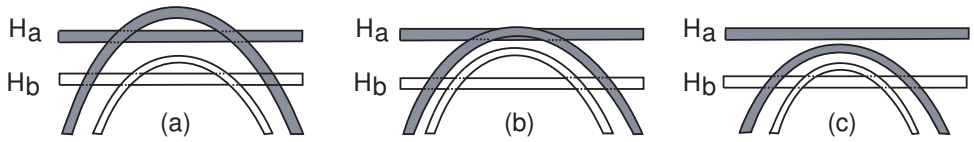

FIGURE 9. Strips in Proposition 16: (a) $\lambda = \lambda_3$; (b) $\lambda = \lambda_2$; (c) $\lambda = \lambda_1$. The position of the horizontal strips $\mathcal{H}_a$ and $\mathcal{H}_b$ does not depend on λ. The maximum height of the horseshoe strips $R_\lambda(\mathcal{H}_a)$ and $R_\lambda(\mathcal{H}_b)$ decreases when λ decreases, and the suspended horseshoe in $R_\lambda(\mathcal{H}_a) \cap \mathcal{H}_a$ is destroyed.

6.3. **Irregular intersections of strips.** The horizontal strips $\mathcal{H}_n$ that comprise $\eta^{-1}(\mathcal{S}_\mathbf{w}) \cap \mathcal{S}_\mathbf{v}$ do not depend on the bifurcation parameter λ, as shown in Lemmas 12 and 13. This is in contrast with the strong dependence on λ shown by the first return of these points to $\mathcal{S}_\mathbf{v}$ at the horseshoe strips $R_\lambda(\mathcal{H}_n)$. In particular, the values of $n_0(\lambda)$ (Lemma 14) and $N(\lambda)$ (Lemma 15) vary with the choice of λ. For a small fixed $\lambda > 0$ and for $m, n \geq N(\lambda)$ we have shown that $\mathcal{H}_n$ and $R_\lambda(\mathcal{H}_m)$ intersect regularly.

The next result describes the bifurcations of these sets when λ decreases. These global bifurcations have been described by Palis and Takens in [29] in a different context, where the horseshoe strips are translated down as a parameter varies. In our case, when λ goes to zero the horseshoe strips are flattened into the common invariant manifold of $\mathbf{v}$ and $\mathbf{w}$.

Proposition 16. *Given $\lambda_3 > 0$ sufficiently small, there exist $\lambda_1 < \lambda_2 < \lambda_3 \in \mathbf{R}^+$, a horizontal strip $\mathcal{H}_a$ across $\mathcal{S}_\mathbf{v} \subset In^+(\mathbf{v})$ and $b_0 > a$ such that for any $b > b_0$ the horizontal strips $\mathcal{H}_a$ and $\mathcal{H}_b$ satisfy:*

1. *for $\lambda = \lambda_3$ the sets $\mathcal{H}_i$ and $R_{\lambda_3}(\mathcal{H}_j)$ intersect regularly for $i, j \in \{a, b\}$;*
2. *for $\lambda = \lambda_2$ the intersection $\mathcal{H}_a \cap R_{\lambda_2}(\mathcal{H}_a)$ is irregular;*
3. *for $\lambda = \lambda_1$ the sets $\mathcal{H}_a$ and $R_{\lambda_1}(\mathcal{H}_a)$ do not intersect at al;*
4. *for $\lambda = \lambda_1$ and $\lambda = \lambda_2$ the set $R_\lambda(\mathcal{H}_b)$ intersects both $\mathcal{H}_b$ and $\mathcal{H}_a$ regularly.*

Proof. As we have remarked before, the horizontal strips $\mathcal{H}_n$ do not depend on the parameter λ. In particular, they are well defined for $\lambda = 0$. Their image by the return map R_0 is no longer a horseshoe strip, it is a horizontal strip across $\mathcal{S}_\mathbf{v}$. Since for $\lambda = 0$ the map $\Psi^0_{\mathbf{w}\to\mathbf{v}}$ is the identity (see 4.5) and the network is asymptotically stable, it follows that the maximum height of $R_0(\mathcal{H}_n)$ is no more than that of $\eta(\mathcal{H}_n)$.

From Lemma 13 and the expressions (6.6) and (6.7) for the maximum, h_n, and minimum m_n, height of $\mathcal{H}_n$, we get that the maximum height h_n^δ of $\eta(\mathcal{H}_n)$ is less than m_n if

$$L_n = \delta(P^1_\mathbf{v} - P^2_\mathbf{w}) + 2\tau(\delta - 1) - 2n\pi(\delta - 1) < P^2_\mathbf{v} - P^1_\mathbf{w}.$$

Since $\lim_{n\to\infty} L_n = -\infty$, there is n_2 such that $R_0(\mathcal{H}_n) \cap \mathcal{H}_n = \emptyset$, for every $n > n_2$. Therefore, since R_λ is continuous on λ, for each $n > n_2$ there is $\lambda_\star(n) > 0$ such that the maximum height of $R_{\lambda(n)}(\mathcal{H}_n)$ is less than that of $\mathcal{H}_n$.

Let $a = \max\{n_1, N(\lambda_3)\}$ for $N(\lambda_3)$ from Lemma 15. Then assertion (1) is true for this $\mathcal{H}_a$ and for any $\mathcal{H}_n$ with $n > a$, by Lemma 15. We obtain assertion (3) by taking $\lambda_1 = \lambda_\star(a)$. Assertion (2) follows from the continuous dependence of R_λ on λ. Assertion (4) holds for any $\mathcal{H}_b$ with $b > N(\lambda_1) = b_0$ by Lemma 15. □

Proof of Theorem 7. In particular, Proposition 16 implies that there exists $d \in [\lambda_2, \lambda_3)$ such that at $\lambda = d$, the lower horizontal boundary of $R_\lambda(\mathcal{H}_a)$ is tangent to the upper horizontal boundary of $\mathcal{H}_a$. Analogously, there exists $c \in (\lambda_1, \lambda_2]$ such that at $\lambda = c$, the upper horizontal boundary of $R_\lambda(\mathcal{H}_a)$ is tangent to the lower horizontal boundary of $\mathcal{H}_a$. There are infinitely many values

of λ in $[c, d]$ for which the map R_λ has a homoclinic tangency associated to a periodic point see [29, 39].

The rigorous formulation of Theorem 7 consists of Proposition 16 , with $\Delta_1 = [c, d]$ as in the remarks above. Since Proposition 16 holds for any $\lambda_3 > 0$, it may be applied again with λ_3 replaced by λ_1, and the argument may be repeated recursively to obtain a sequence of disjoint intervals Δ_n. □

Proof of Corollary 8. The λ dependence of the position of the horseshoe strips is not a translation in our case, but after Proposition 16 the constructions of Yorke and Alligood [39] and of Palis and Takens [29] can be carried over. Hence, when the parameter λ varies between two consecutive regular intersections of strips, the bifurcations of the first return map can be described as the one-dimensional parabola-type map in [29]. Following [39, 29], the bifurcations for $\lambda \in [\lambda_1, \lambda_3]$ are:

- for $\lambda > d$: the restriction of the map R_{λ_3} to the non-wandering set on $\mathcal{H}_a$ is conjugate to the Bernoulli shift of two symbols and it no longer bifurcates as λ increases.
- at $\lambda \in (c, d)$: a fixed point with multiplier equal to ± 1 appears at a tangency of the horizontal boundaries. It undergoes a period-doubling bifurcation. A cascade of period-doubling bifurcations leads to chaotic dynamics which alternates with stability windows and the bifurcations stop at $\lambda = d$;
- at $\lambda < c$: trajectories with initial conditions in $\mathcal{H}_a$ approach the network and might be attracted to another basic set.

□

Proof of Corollary 9. If the first return map R_λ is area-contracting, then the fixed point that appears for $\lambda \in (c, d)$ is attracting for the parameter in an open interval.

This attracting fixed point bifurcates to a sink of period 2 at a bifurcation parameter $\lambda > c$ close to c. This stable orbit undergoes a second flip bifurcation, yielding an orbit of period 4. This process continues to an accumulation point in parameter space at which attracting orbits of period 2^k exist, for all $k \in \mathbf{N}$. This completes the proof of Corollary 9 . □

Finally, we describe a setting in which the fixed point that appears for $\lambda \in (c, d)$ can be shown to be attracting. Recall that the set $W^u_{loc}(\mathbf{w}) \cap In(\mathbf{v})$ is the graph of $y = h_{\mathbf{w}}(x, \lambda)$. Suppose the transition map $\Psi^\lambda_{\mathbf{w}\to\mathbf{v}} : Out(\mathbf{w}) \longrightarrow In(\mathbf{v})$ is given by $\Psi^\lambda_{\mathbf{w}\to\mathbf{v}}(x, y) = (x, y + h_{\mathbf{w}}(x, \lambda))$. Since

$$D\Psi^\lambda_{\mathbf{w}\to\mathbf{v}}(x, y) = \begin{pmatrix} 1 & 0 \\ \frac{\partial h_{\mathbf{w}}}{\partial x}(x) & 1 \end{pmatrix} \quad \text{and} \quad D\eta(x, y) = \begin{pmatrix} 1 & \dfrac{-K}{y} \\ 0 & \delta y^{\delta-1} \end{pmatrix}$$

then $\det DR_\lambda(x, y) = \det D\Psi^\lambda_{\mathbf{w}\to\mathbf{v}}(\eta(x, y)) \cdot \det D\eta(x, y) = \delta y^{\delta-1}$. For sufficiently small y (in $\mathcal{H}_n$ with sufficiently large n) this is less than 1, and hence R_λ is contracting. However, if the first coordinate of $\Psi^\lambda_{\mathbf{w}\to\mathbf{v}}(x, y)$ depends on y, then $\det D\Psi^\lambda_{\mathbf{w}\to\mathbf{v}}(\eta(x, y))$ will contain terms that depend on $x + K \ln y$ and a more careful analysis will be required.

References

[1] V.S. Afraimovich, L.P. Shilnikov, *Strange attractors and quasiattractors*, in: G.I. Barenblatt, G. Iooss, D.D. Joseph (Eds.), Nonlinear Dynamics and Turbulence, Pitman, Boston, 1–51, 1983

[2] M.A.D. Aguiar, S.B.S.D. Castro and I.S. Labouriau, *Dynamics near a heteroclinic network,* Nonlinearity, No. 18, 391–414, 2005

[3] M.A.D. Aguiar, S.B.S.D. Castro and I.S. Labouriau, *Simple Vector Fields with Complex Behaviour*, Int. J. Bif. Chaos, Vol. 16, No. 2, 369–381, 2006

[4] M.A.D. Aguiar, I. S. Labouriau, A. Rodrigues, *Switching near a heteroclinic network of rotating nodes*, Dynamical Systems, Vol. 25, 1, 75–95, 2010
[5] D. Armbruster, J. Guckenheimer, P. Holmes, *Heteroclinic cycles and modulated travelling waves in systems with O(2) symmetry*, Physica D, No. 29, 257–282, 1988
[6] R. Bowen, *Equilibrium States and the Ergodic Theory of Anosov Diffeomorphisms*, Lect. Notes in Math, Springer, 1975
[7] D.R.J. Chillingworth,*Generic multiparametere bifurcation from a manifold*, Dynamical Systems, Vol. 15, 2, 101–137, 2000
[8] E. Colli, *Infinitely many coexisting strange attractors*, Ann. Inst. H. Poincaré, Anal. Non Linéaire, 15, 539–579, 1998
[9] F. Dumortier, S. Ibáñez, H. Kokubu, *Cocoon bifurcation in three-dimensional reversible vector fields*, Nonlinearity 19, 305–328, 2006
[10] F. Dumortier, S. Ibáñez, H. Kokubu, C. Simó, *About the unfolding of a Hopf-zero singularity*, Disc. Cont. Dyn. Syst., 33, 10, 4435–4471, 2013
[11] M. Golubitsky, I. Stewart, *The Symmetry Perspective*, Birkhauser, 2000
[12] S.V. Gonchenko, L.P. Shilnikov, D.V. Turaev, *Dynamical phenomena in systems with structurally unstable Poincaré homoclinic orbits*, Chaos 6, No. 1, 15–31, 1996
[13] S.V. Gonchenko, L.P. Shilnikov, D.V. Turaev, *Quasiattractors and Homoclinic Tangencies*, Computers Math. Applic. Vol. 34, No. 2-4, 195–227, 1997
[14] S.V. Gonchenko, I.I. Ovsyannikov, D.V. Turaev, *On the effect of invisibility of stable periodic orbits at homoclinic bifurcations*, Physica D, 241, 1115–1122, 2012
[15] J. Guckenheimer, P. Holmes, *Nonlinear and Bifurcations of Vector Fields*, Applied Mathematical Sciences, No. 42, Springer-Verlag, 1983
[16] A.J. Homburg, B. Sandstede, *Homoclinic and Heteroclinic Bifurcations in Vector Fields*, Handbook of Dynamical Systems, Vol. 3, North Holland, Amsterdam, 379–524, 2010
[17] S. Kiriki, T. Soma, *Existence of generic cubic homoclinic tangencies for Hénon maps*, Ergodic Theory and Dynamical Systems, 33, 1029–1051, 2013
[18] V. Kirk, A.M. Rucklidge, *The effect of symmetry breaking on the dynamics near a structurally stable heteroclinic cycle between equilibria and a periodic orbit*, Dyn. Syst. Int. J. 23, 43–74, 2008
[19] J. Knobloch, J.S.W. Lamb, K. N. Webster, *Using Lin's method to solve Bykov's problems*, J. Diff. Eqs., 257(8), 2984–3047, 2014
[20] M. Krupa, I. Melbourne, *Asymptotic Stability of Heteroclinic Cycles in Systems with Symmetry II,* Ergodic Theory and Dynam. Sys., Vol. 15, 121–147, 1995
[21] I.S. Labouriau, A.A.P. Rodrigues, *Global generic dynamics close to symmetry*, J. Diff. Eqs., Vol. 253 (8), 2527–2557, 2012
[22] I.S. Labouriau, A.A.P. Rodrigues, *Partial symmetry breaking and heteroclinic tangencies*, in S. Ibáñez, J.S. Pérez del Río, A. Pumariño and J.A. Rodríguez (eds), Progress and challenges in dynamical systems, 281–299, 2013
[23] I.S. Labouriau, A.A.P. Rodrigues, *Dense heteroclinic tangencies near a Bykov cycle*, preprint n. 2014–4, arXiv: 1402.5455, 2014
[24] J.S.W. Lamb, M.A. Teixeira, K.N. Webster, *Heteroclinic bifurcations near Hopf-zero bifurcation in reversible vector fields in* $\boldsymbol{R}^3$, J. Diff. Eqs., 219, 78–115, 2005
[25] I. Melbourne, M.R.E. Proctor and A.M. Rucklidge, *A heteroclinic model of geodynamo reversals and excursions*, Dynamo and Dynamics, a Mathematical Challenge (eds. P. Chossat, D. Armbruster and I. Oprea, Kluwer: Dordrecht, 363–370, 2001
[26] L. Mora, M. Viana, *Abundance of strange attractors*, Acta Math. 171, 1–71, 1993
[27] S.E. Newhouse, *Diffeomorphisms with infinitely many sinks*, Topology 13 9–18, 1974
[28] S.E. Newhouse, *The abundance of wild hyperbolic sets and non-smooth stable sets for diffeomorphisms*, Publ. Math. Inst. Hautes Etudes Sci. 50, 101–151, 1979
[29] J. Palis, F. Takens, *Hyperbolicity and sensitive chaotic dynamics at homoclinic bifurcations*, Cambridge University Press, Cambridge Studies in Advanced Mathematics 35, 1993.
[30] A.A.P. Rodrigues, *Persistent Switching near a Heteroclinic Model for the Geodynamo Problem*, Chaos, Solitons & Fractals, 47, 73–86, 2013
[31] A.A.P. Rodrigues, *Repelling dynamics near a Bykov cycle*, J. Dyn. Diff. Eqs., Vol.25, Issue 3, 605–625, 2013
[32] A.A.P. Rodrigues, *Moduli for heteroclinic connections involving saddle-foci and periodic solutions*, Discrete Contin. Dyn. Syst. A, to appear, 2015

[33] A.A.P. Rodrigues, I.S. Labouriau, *Spiralling dynamics near heteroclinic networks*, Physica D, 268, 34-49, 2014
[34] A. M. Rucklidge, *Chaos in a low-order model of magnetoconvection*, Physica D 62, 323– 337, 1993
[35] V.S. Samovol, *Linearisation of a system of differential equations in the neighbourhood of a singular point,* Sov. Math. Dokl, Vol. 13, 1255–1959, 1972
[36] L.P. Shilnikov, *A case of the existence of a denumerable set of periodic motions*, Sov. Math. Dokl, No. 6, 163–166, 1965
[37] L.P. Shilnikov, *On a Poincaré-Birkhoff problem*, Math. USSR Sb. 3, 353–371, 1967
[38] L.P. Shilnikov, *The existence of a denumerable set of periodic motions in four dimensional space in an extended neighbourhood of a saddle-focus*, Sov. Math. Dokl., 8(1), 54–58, 1967
[39] J. A. Yorke, K. T. Alligood, *Cascades of period-doubling bifurcations: A prerequisite for horseshoes*, Bull. Am. Math. Soc. (N.S.) 9(3), 319–322, 1983

Centro de Matemática da Universidade do Porto, and Faculdade de Ciências, Universidade do Porto, Rua do Campo Alegre, 687, 4169-007 Porto, Portugal
E-mail address: I.S. Labouriau islabour@fc.up.pt A.A.P. Rodrigues alexandre.rodrigues@fc.up.pt